Impurity-vacancy complexes in electron-irradiated silicon

V. Avalos and S. Dannefaer
Department of Physics, University of Winnipeg, Winnipeg, Manitoba, R3B 2E9 Canada
(Received 5 December 1997)

A comprehensive study of $\simeq 2.5-10$-MeV electron-irradiated Czochralski Si has been conducted using positron lifetime and Doppler broadening spectroscopies. Eight samples, ranging from heavily doped *n* type to heavily doped *p* type, were irradiated simultaneously at room temperature to facilitate quantitative comparisons between the samples. The influence from the oxygen impurity was also investigated by comparison with oxygen-free Si. For lightly doped materials (dopant concentration less than $5\times10^{16}/\mathrm{cm}^3$) the irradiation damage is dominated by free, and negatively charged divacancies for the dose employed in this work ($1.2\times10^{18}e^-/\mathrm{cm}^2$). For the heavily doped materials (dopant concentrations larger than $5\times10^{17}/\mathrm{cm}^3$) vacancy-dopant complexes dominate, some of which involve divacancies, and in these samples very high introduction rates ($1-4\ \mathrm{cm}^{-1}$) are estimated. In heavily B-doped materials evidence is found for thermally activated trapping by boron divacancy complexes. Association of divacancies with P, Sb, and B dopants was found to modify significantly the Doppler *S* parameter relative to the value for free divacancies.
[S0163-1829(98)01227-2]

I. INTRODUCTION

Irradiation of silicon leads to the formation of vacancies and interstitials. At room temperature these fundamental defects are mobile and many will recombine, but some will remain formed by migrating monovacancies as well as directly by the irradiation, and divacancies are immobile at room temperature. Numerous studies have been conducted to elucidate the character of complexes, but the majority with vacancy-associated complexes (divacancies,[1,2] P monovacancy,[3] B monovacancy[4,5] and O multivacancy[6]) whereas only one form of pure interstitials (the di-interstitial[7]) and one form of carbon-interstitial complex have been reported on.[8] Corbett[9] reviewed data obtained mainly from electron paramagnetic resonance (EPR) while Lindström and Svensson[10] focused on results obtained by infrared (IR) spectroscopy. The literature is extensive, but it appears that a systematic investigation of samples with a wide range of dopant concentrations irradiated under identical conditions has not been reported. Furthermore, high dopant concentrations have been excluded because EPR and IR measurements are not feasible for experimental reasons.

Former positron works on electron irradiated Si include an investigation by Mascher, Dannefaer, and Kerr,[11] who demonstrated that the trapping of positrons depends markedly on the charge of vacancies. Mäkinen *et al.*[12] investigated in detail the monovacancy and the phosphorous monovacancy complex,[13] and Kawasuso *et al.*[14] and Chiba *et al.*[15] focused mainly on divacancies.

In this work we have employed positron annihilation (and in a few cases Fourier transform infrared spectroscopy) to investigate vacancies formed by electron irradiation, taking advantage of the fact that highly doped materials can also be investigated by positron annihilation. The aim of this work is mainly to assess the influence from doping on vacancy production by comparing results for variously doped samples irradiated under identical conditions. We have employed both positron lifetime spectroscopy and Doppler broadening, where the former technique is forceful in distinguishing between different vacancy sizes while the latter is particularly useful in revealing effects arising from complexing of vacancies with impurities. One main finding from this work is that dopants at high concentrations enhance significantly the concentration of vacancies by reducing recombination with interstitials and that dopant-vacancy complexes dominate in such materials.

II. EXPERIMENT

A. Samples

The samples were cut from Czochralski-grown wafers (Cz-Si) doped as listed in Table I. The letter(s) in the codes for each sample signifies the dopant type while the number indicates, on a scale of 0–4, increasing dopant concentrations. These codes will be used in figures displaying the results. The samples were in the form of bars of dimensions

TABLE I. Sample characteristics. For easy identification of dopant concentration larger numbers in the sample codes reflect larger impurity concentration.

Sample code	Dopant and type	Impurities/cm^3	Resistivity (Ω cm)
P4	P(n)	5×10^{18}	0.01
P3	P(n)	5×10^{17}	0.1–0.2
P2	P(n)	5×10^{16}	1–2
P1	P(n)	2×10^{16}	3
Sb4	Sb(n)	1×10^{18}	0.01
B4	B(p)	5×10^{18}	0.01
B3	B(p)	5×10^{17}	0.1
B0	B(p)	4×10^{14}	100
Fz	none		$\sim$2000

$4\times0.5\times30\ \mathrm{mm}^3$ and were irradiated along the long axis with 10-MeV electrons using a pulsed beam (240 pulses/s each of 3 ms duration) with an average current density of 4.5 μA/cm^2. The dose at the beam-facing end of the samples was $1.2\times10^{18}e^-/\mathrm{cm}^2$. The samples were irradiated simultaneously and were cooled by water at 8 °C and were spaced by $\frac{1}{2}$ mm to allow for free-water-flow. After irradiation the samples were stored at -18 °C until commencement of the positron measurements.

B. Measurements

The positron lifetime measurements were done using a spectrometer with a prompt width of 200 ps at full width at half maximum. Each lifetime spectrum contained 4×10^6 counts for low-temperature measurements (repeated twice over 20 h) while those obtained at room temperature contained $(6-10)\times10^6$ counts (and repeated thrice over 18 h). The 24 h time stability of the spectrometers was better than ±2 ps as achieved by close temperature regulation (±0.1 °C) of all electronic components *including* the ORTEC multichannel boards situated inside the computer. These experimental conditions make possible separation of individual lifetime components when they differ in excess of ~50 ps.

The source correction consisted of a 250 ps lifetime component with an intensity of 2% arising from the 0.8 μm-thick Al foil that enveloped the source (of strength 13 μCi) as prepared according to a newly developed prescription (described in Ref. 16). It is noteworthy that for such sources the usually encountered 1.5-ns ''tail'' lifetime component is absent, which, apart from indicating that this component is source-preparation related, simplifies numerical analyses. Excluding the source correction had, to within statistical error, no effect on the results.

Doppler broadened energy spectra were obtained with an energy resolution of 1.2 keV using a 5% efficient intrinsic Ge detector operated at a count rate of 2 kHz. Each spectrum contained 2×10^6 counts within the annihilation peak and was repeated five times during a time period of 20 h. All reported lifetime and Doppler data are averages of the individual results, and indicated errors take into account the multiplicity of the measurements.

C. Positron annihilation

When vacancies trap positrons their lifetime is increased relative to the bulk value (i.e., that for nontrapped positrons) due to the smaller average electron density which makes possible the observation of vacancies by means of positron annihilation. The trapping rate of the positrons is proportional to the vacancy concentration according to

$$\kappa=\mu C_V, \tag{1}$$

where μ is the absolute specific trapping rate ($\mathrm{ns}^{-1}\,\mathrm{cm}^3$) and C_V is the absolute vacancy concentration (cm^{-3}). The absolute specific trapping rate is strongly temperature dependent for negatively charged vacancies (large at low temperatures) while essentially temperature independent for neutral vacancies. For positively charged vacancies (or complexes) the specific trapping rate is estimated to be $\frac{1}{10}$ (or less) of that for neutral defects (due to Coulomb repulsion) at room temperature and decreases with decreasing temperature; these are very helpful features in assessing the charge state of free vacancies (or vacancy-impurity complexes).

The trapping rate is a central parameter but is *not* determined directly by analyses of the lifetime spectra that yield lifetime values and their associated intensities. To determine the trapping rate one can employ the trapping model[17] from which the trapping rate can be calculated from experimentally obtained parameters according to

$$\kappa=I_2(1/\tau_B-1/\tau_2)/(1-I_2), \tag{2}$$

where τ_2 is the lifetime for positrons trapped by vacancies, I_2 is the intensity of τ_2, and τ_B is the bulk lifetime. As pointed out in Ref. 18, in which a more thorough discussion of the trapping model can be found, applicability of the model can be gauged by the trapping-model-based equation

$$1/\tau_B=\sum_{i=1}^{2} I_i/\tau_i\,. \tag{3}$$

The τ_1 lifetime arises from annihilations in the bulk but its value is smaller than the bulk lifetime because trapping into vacancies additionally removes positrons from the bulk state in which all positrons initially reside: $\tau_1=(1/\tau_B+\kappa)^{-1}$. For Si, τ_B has been established at 217 ± 2 ps,[13,16] and for all cases except for one irradiated sample (P4) this value was found to within ±3 ps as calculated from Eq. (3). We conclude, therefore, that the trapping model is applicable in this work.

The Doppler-broadened energy spectrum of the 511-keV annihilation quanta reflects the momentum distribution of valence and core electrons in the immediate vicinity of the positron. Because the energy spectrum is severely influenced by the energy resolution of the detector system (1.2 keV) a crude (but nevertheless statistically well-determined) parameter is commonly used to characterize the overall electron momentum distribution, namely, the S parameter. S is determined by the number of counts within a symmetrically positioned energy range of 511 ± 0.7 keV (in our case) divided by the counts within the 511 ± 4.8 keV range that, after background correction, incorporates nearly all of the counts within the bell-shaped Doppler spectrum. Because of the arbitrariness in the definition of S, only the ratio S/S_B has comparative relevance, where S_B pertains to the bulk. Since values of the S parameter are subject to experimental conditions such as whether the samples are situated inside a cryostat or not and to changes in the width of the resolution function, care was taken to ensure that reference measurements, to determine S_B, were made under the same conditions as those for the irradiated samples.

III. RESULTS

A. Temperature dependencies

Lifetime and Doppler results for unirradiated samples are listed in Table II. The lifetime data reveal a vacancy-cluster lifetime τ_2 with a fairly low intensity I_2, and such a weak contribution has been observed earlier.[19] Consequently, S values do not strictly correspond to the bulk value, but we

TABLE II. Lifetime (τ_1, τ_2, and I_2) and Doppler data (S) for unirradiated samples. The bottom entry in this table (Fz) refers to a float zone refine sample with an oxygen concentration about 100 times less than for the other samples. The trapping rate κ_2 and the bulk lifetime τ_B were calculated from Eqs. (2) and (3), respectively. Data are shown for measurements at room temperature, and are, within error, identical to those obtained at 30 K.

Sample	τ_1 (ps)	τ_2 (ps)	I_2 (%)	τ_B (ps)	κ_2 (ns^{-1})	S
P4	214±1	449±17	3±1	218±3	0.07±0.02	0.5059±0.0003
P3	213±1	406±14	4±1	217	0.09	0.5059±0.0003
P2	212±1	394±12	5±1	217.5	0.11	0.5045±0.0003
P1	213±1	420±11	5±1	218	0.10	0.5063±0.0007
Sb4	213±1	407±14	4±1	217.5	0.09	0.5049±0.0007
B4	214±1	421±16	3±1	217.5	0.07	0.5035±0.0007
B3	213±1	416±15	4±1	217	0.09	0.5049±0.0003
B0	212±1	409±11	5±1	217	0.10	0.5062±0.0004
Fz	210±3	336±22	10±3	217	0.17	0.5096±0.0006

will nevertheless use them as such because of the small fraction ($\leqslant 0.04$) of positrons trapped by grown-in defects.

Lifetime results for the n-type irradiated samples are shown in Fig. 1. The samples were cut from the front end of the bars (and hence irradiated with 10-MeV electrons to the dose of $1.2\times10^{18}/cm^2$). In this figure (and others to follow) we show, for the sake of brevity, only the important irradiation-produced lifetime τ and its associated trapping rate κ as calculated using Eq. (2); it should be noted that these two parameters include the small contribution from the defects already present before the irradiation.

The samples show quite different temperature dependencies. For the two lightly P-doped samples (P1 and P2) τ increases with temperature while κ decreases strongly, which are characteristics very similar to those observed in electron irradiated oxygen-free undoped Si (Fz-Si), where they were shown to arise from trapping by negatively charged divacancies.[16]

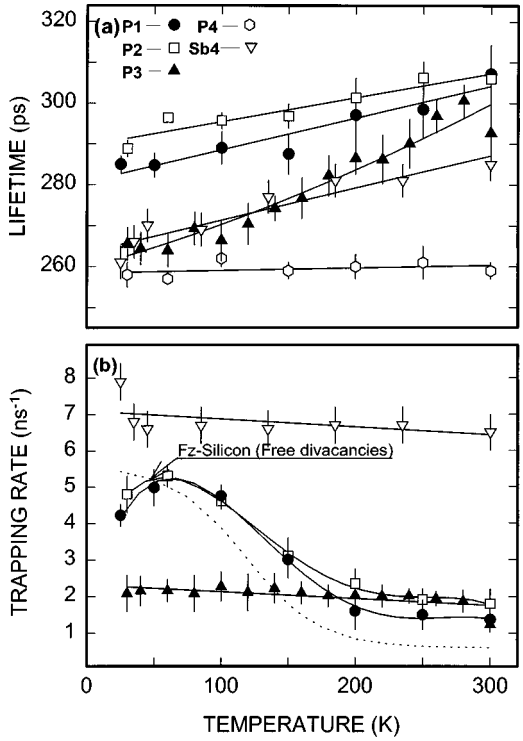

FIG. 1. Irradiation-produced positron lifetimes and trapping rates for n-type materials as a function of sample temperature. The sample codes are those listed in Table I. The broken curve in panel (b) is for free negatively charged divacancies in Fz-Si, from Ref. 16. The trapping rate for the P4 was too high to be calculable.

For the medium P-doped sample (P3), τ increases significantly with temperature whereas the trapping rate is essentially constant (at 2 ns^{-1}). The lifetimes cover the range between monovacancies ($\simeq$270 ps) and divacancies ($\simeq$300 ps).

For the highly doped P4 sample, τ is constant (at 260 ±3 ps), but the trapping rate cannot be calculated because the bulk-associated component τ_1 is too small to be resolved for any of the lifetime spectra in the temperature range investigated. Nonobservability of τ_1 requires at our experimental conditions that $\tau_1<80$ ps, which means that the trapping rate would be at least $\sim$8 ns^{-1}.

For the Sb-doped sample the lifetime is smaller (by $\sim$20 ps) relative to the P1 and P2 samples, but has the same temperature dependence. The trapping rate is essentially temperature independent, just as for the P3 sample, but is significantly larger.

The temperature dependencies of the Doppler S parameter are shown in Fig. 2(a) for the P3, P4, and Sb4 samples (P1 and P2 were not investigated because the lifetime data were very similar to the Fz-Si samples for which the S parameter was also measured[16]). For the P3 and Sb4 samples, where trapping rates can be calculated, the defect-specific ratio S_D/S_B can be obtained from

$$S=(1-\alpha)S_B+\alpha S_D, \tag{4}$$

giving

$$S_D/S_B=(S/S_B+\alpha-1)/\alpha, \tag{5}$$

where the trapped fraction of positrons α is given by

$$\alpha=\kappa/(\kappa+\lambda_B). \tag{6}$$

In these equations S_B is the bulk S value, S_D is the defect-characteristic S parameter, and λ_B is the bulk annihilation rate ($\equiv 1/\tau_B$). S_D/S_B values for the P3, P4, and Sb4 samples are shown in Fig. 2(b). In this context it is worth noting that lifetime and Doppler parameters are sensitive to vacancies in

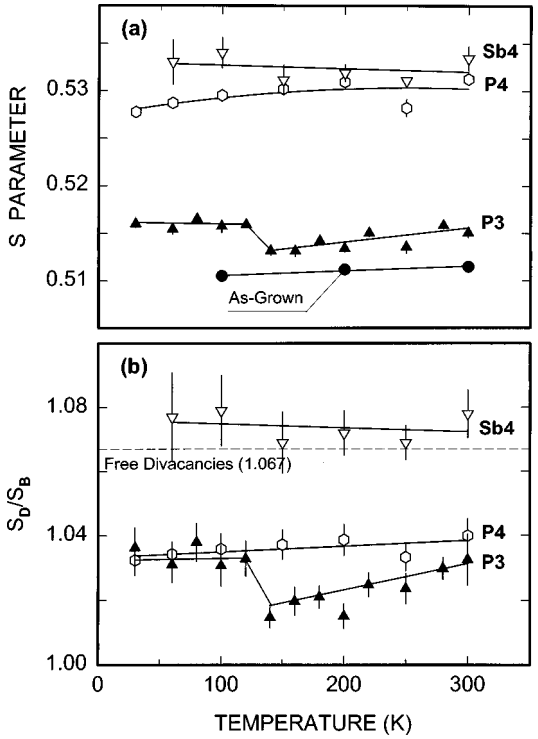

FIG. 2. (a) Doppler S parameter for the irradiated n-type P3, P4, and Sb4 samples as a function of sample temperature and a representative unirradiated sample. (b) Defect-specific ratio S_D/S_B as calculated from Eq. (5). The broken line indicates S_D/S_B from Ref. 16 for free negatively charged divacancies.

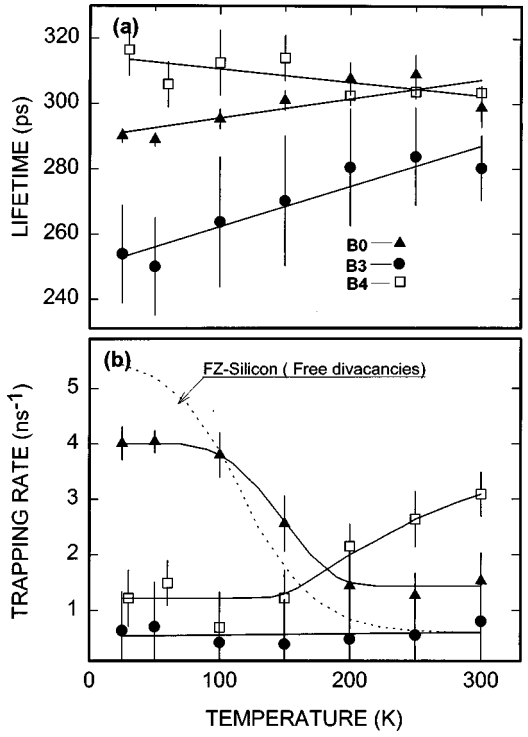

FIG. 3. Irradiation-produced positron lifetimes and trapping rates for p-type materials (see Table I for sample identifications). In panel (b) the broken curve shows the results for Fz-Si (Ref. 16).

widely different regimes of trapping rates. Lifetime data are sensitive at most to a trapping rate of $\sim 8\ \mathrm{ns}^{-1}$, whereas S is sensitive to $\sim 45\ \mathrm{ns}^{-1}$, corresponding to a fraction of 90% being trapped.

For the P4 sample it is not possible to calculate S_D/S_B using the above procedure. However, we have reason to believe that the trapped fraction of positrons is close to one as based on Doppler data to be presented later (Sec. III B, Fig. 7) and obtain thus values of S_D/S_B as shown in Fig. 2(b). The P3 and P4 samples have nearly the same values of S_D/S_B that are significantly lower than that for free divacancies (1.067 ± 0.005);[16] for the Sb-doped sample S_D/S_B is marginally larger than for free divacancies.

Turning to the results for the p-type material, Fig. 3 depicts lifetime results for the boron-doped materials. The data for the lightly doped sample (B0) are very similar to those for the lightly doped P1 and P2 samples (and the Fz-Si sample). The medium-doped B3 sample has a small trapping rate $(0.7\ \mathrm{ns}^{-1})$, which makes the determination of the lifetime rather uncertain. The highly doped B4 sample is unique in showing a trapping rate that *increases* with temperature above 150 K.

The Doppler data for the B3 and B4 samples are shown in Fig. 4(a) (B0 was not investigated for the same reason as in the cases of the P1 and P2 samples). The S parameters for the B3 sample are very close to the reference values that are commensurate with the small trapping rate that makes a calculation of S_D/S_B too uncertain to be of value. For the B4 sample S_D/S_B can be calculated and values [see Fig. 4(b)] are below the free negatively charged divacancy value of 1.067 ± 0.005.

The results described above suggest that doping at concentrations of $5 \times 10^{17}/\mathrm{cm}^3$ or above influences substantially the temperature dependencies of the positron parameters relative to those for free divacancies, indicating that impurity-vacancy complexes are of importance.

B. Location-dependent measurements

In this section we present results obtained mostly at *room* temperature for different locations on the irradiated bars. The

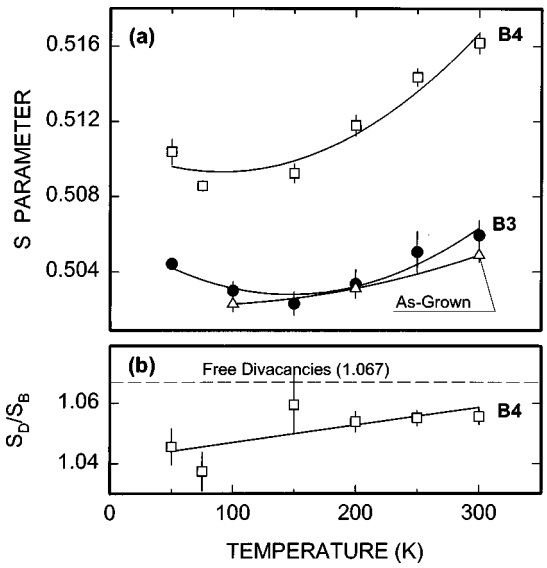

FIG. 4. (a) S parameters for the B3 and B4 samples and a representative unirradiated sample. Because of the small effect from irradiation on the B3 sample only the defect-specific S_D/S_B parameter was calculated for the B4 sample [panel (b)].

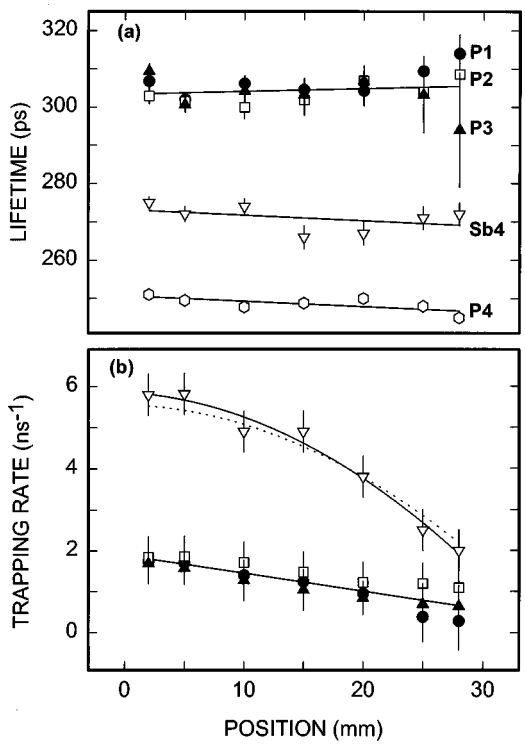

FIG. 5. Irradiation-produced positron lifetimes and trapping rates (obtained at 295 K) as a function of location along the *n*-type sample bars. The trapping rate for the P4 sample was too high to be calculable. In (b) the dotted line superimposed on data for the Sb4 sample displays the expected dose variation with location as calculated from electron dosimetry data.

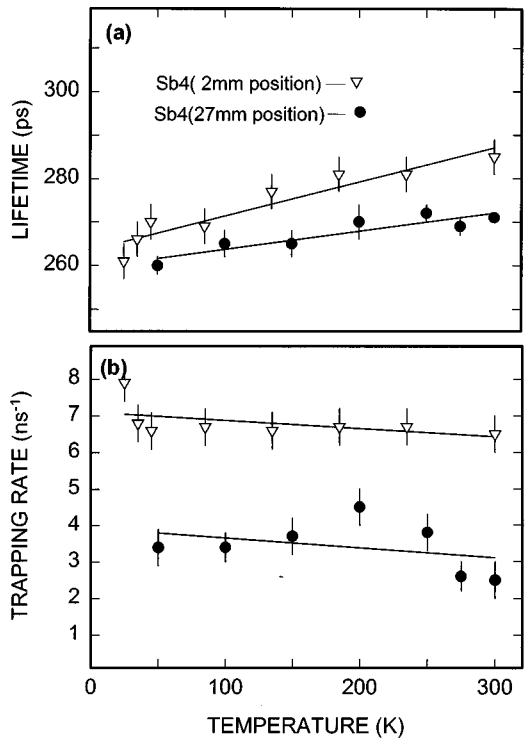

FIG. 6. Irradiation-produced positron lifetime and trapping rate as a function of temperature for the Sb4 sample measured at the 2 mm location and the 27 mm location of the sample bar.

location ''zero'' in Figs. 5–9 signifies the electron entry end. The furthest location down the bars is located at 27 mm at which point the calculated *mean* electron-energy has decreased (linearly) to 2.5 MeV when taking into account the mixed cross-sectional nature of the sample assembly, i.e., 50% water and 50% silicon bars.[20] Not only does the energy of the electrons degrade along the bars, but the dose also decreases due to fan-out of the beam.

In Fig. 5 are shown lifetime results for *n*-type samples. For all of the samples the lifetimes are essentially independent of position, and the trapping rates decrease smoothly along the bars from the front to the back end. For the highly doped P4 sample the trapping rate is too high to permit a calculation of its value regardless of location. In the case of the Sb4 sample the experimentally determined trapping rates are large enough to make possible a comparison with electron dosimetry. Using data from Ref. 20 the fan-out of the electron beam can be calculated as a function of location, yielding the shape of the trapping rate curve based on dosimetry data as depicted by the dotted line in Fig. 5(b). The agreement is very good and shows that the trapping rate obtained from positron annihilation data is determined mainly by the dose while little influenced by the electron energy. For the Sb4 sample the temperature dependence of the irradiation-produced lifetime and its trapping rate were also investigated at the end of the bar. In Fig. 6 data are compared for two locations, with data for the front (2 mm) location reproduced from Fig. 1. Trapping rates show the same slight temperature dependency indicating that the vacancies are in identical charge states, but the lifetime values are consistently lower for the 27 mm position.

The *S* parameter was also investigated but only for three locations. The results in Fig. 7(a) (expectedly) show a gradual decrease in *S* for all samples *except* for the highly doped P4 sample at least for the first 15 mm of the bar. Using the reference *S* values in Table II and the lifetime data from Fig. 5, the defect-specific S_D/S_B parameter can be calculated [see Fig. 7(b)]. The near-constancy of *S* for the P4 sample suggests essentially complete trapping in this sample, so S_D/S_B was calculated with the trapped fraction α equal to one.

For the *p*-type materials, for which lifetime data are shown in Fig. 8 and Doppler data in Fig. 9, location-independent lifetimes were observed while trapping rates decreased (for the B3 sample we have again omitted calculation of S_D/S_B due to the low trapping rate); there is in this regard no difference between *n*- and *p*-type materials.

This concludes the presentation of the positron results from which emerges the general observation that electron energies in the $\approx$2.5–10-MeV energy range and dose ranges between $\approx 0.6\times10^{18}$ and 1.2×10^{18} e^-/cm^2, although influencing the concentration of defects, have little effect on the types of defects created.

In addition to the positron experiments, infrared absorption experiments were also performed at room temperature. These were possible for the P1, P2, and P3 samples and the B0 and B3 samples, but not for the P4, B4, and Sb4 samples due to high free carrier absorption even after irradiation. The neutral oxygen-vacancy complex (the *A* center which, essentially, is a substitutional oxygen atom) was found in all cases (absorption at 830 cm^{-1}) although in the case of the P3

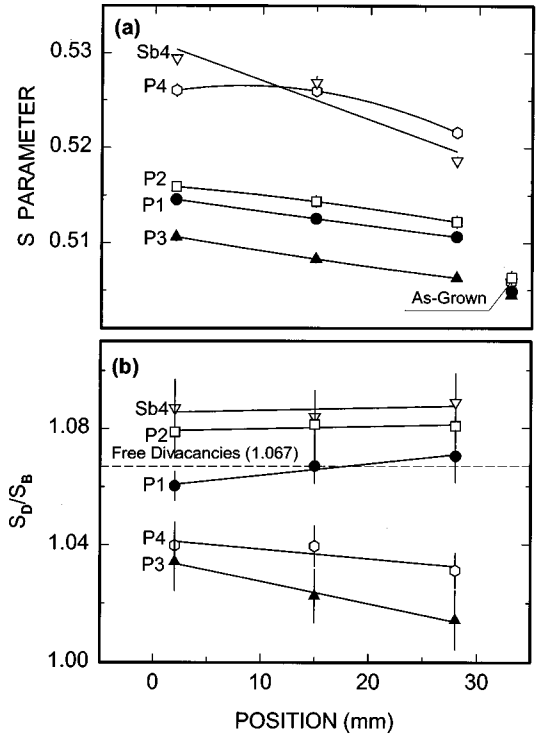

FIG. 7. (a) S parameter data (obtained at 295 K) for three different locations along the irradiated n-type sample bars. Values of S for unirradiated samples are shown at the extreme right. The straight lines connecting the S parameter data are only intended as a guide for the eye and are somewhat misleading insofar that a downward curvature is more likely as expected from electron dosimetry. (b) Defect-specific values of S_D/S_B for the various samples together with (broken horizontal line) that for free divacancies.

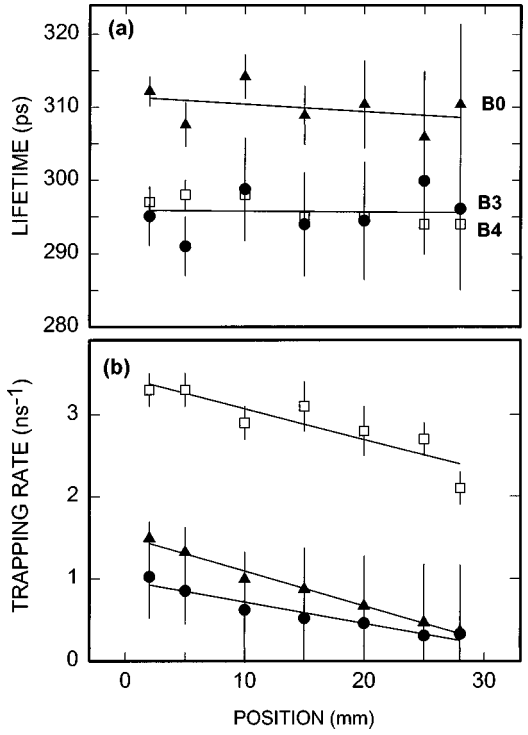

FIG. 8. Text as for Fig. 5 but for the p-type samples.

sample there was also a weak absorption at 877 cm^{-1} that arises from negatively charged A centers.[10] These absorption bands were not observed in oxygen-free Si.

Table III lists areas of the 830-cm^{-1} absorption band as calculated in the 820–870-cm^{-1} range after subtraction of the background absorption. Unfortunately, the 830 cm^{-1} band is situated on a rapidly changing background absorption differing from sample to sample that makes impossible assessment of trends as a function of position. For this reason we list results averaged over five locations equidistantly placed between 5 and 25 mm along the sample bars. Since the area of the absorption band is proportional to the A center concentration, we can conclude that in the lightly doped P1, P2, and B0 samples the same A center concentration (to within $\pm 10\%$) was formed while for the more heavily doped P3 and B3 samples fewer (by nearly 30%) were formed; this indicates that dopants compete with oxygen in trapping mobile monovacancies.

Infrared absorption arising from divacancies was also measured (at room temperature). Divacancies give rise to three absorption bands,[21] one at 1.8 μm arising from V_2^+, V_2^0, and V_2^-, one at 3.3 μm due to V_2^{2-} and one at 3.9 μm due to V_2^+. In none of the P3, B0, and B3 samples could the latter two absorption bands be found (see Fig. 10 for the case of the B3 sample) ruling out V_2^{2-} in the P3 sample and V_2^+ in the B0 and B3 samples.

The 1.8-μm bands for the three samples are shown in Fig. 11 and they differ in strength even though the samples were irradiated to the same dose. To quantify their relative strengths the areas in the 1.63–1.98-μm range were calculated (after linear background subtraction) and normalized to that for the Fz-Si sample[16] (irradiated to the same dose). Likewise we have calculated the trapping rates relative to the Fz-Si sample, and these results are listed in Table IV. In the cases of the P3 and B0 samples optical and positron data scale fairly well, but are clearly deviant in the case of B3. This is an important observation and will be discussed in Sec. IV A.

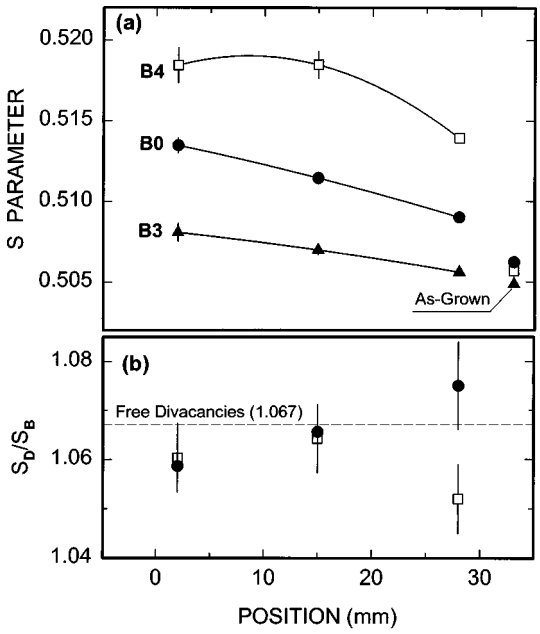

FIG. 9. Text as for Fig. 7 but for the p-type samples.

TABLE III. Infrared absorption (arbitrary units) of the 830-cm^{-1} band as integrated over the range 820–870 cm^{-1}. For the P4, Sb4, and B4 samples the free carrier concentrations were too high for infrared measurements.

Sample code	Absorption (arb. units)
P1	12.4±1
P2	11.1±1
P3[a]	8.5±1
B0	13.0±1
B3	9.2±1

[a]A weak additional absorption due to A^- centers was also observed.

IV. DISCUSSION

The discussion is divided into three sections: Sec. IV A deals with the low temperature results, Sec. IV B deals mainly with the influences from dopants on vacancy introduction rates, and in Sec. IV C the location-dependent results are briefly discussed.

A. Temperature dependencies

In this section we discuss the temperature dependencies of lifetime and Doppler data. The trapping rates for the lightly doped P1, P2 samples (see Fig. 1) and the B0 sample (Fig. 3) are, though not identical, similar to those for undoped oxygen-free Fz-Si,[16] indicating that dopant concentrations below $5\times10^{16}/cm^3$ have no effect on the charge of the divacancies; these divacancies are negatively charged and are not associated with impurities.

Despite the qualitative agreement (i.e., temperature dependency) with the Fz-Si data there is a quantitative disagreement insofar that oxygen causes an increase in the trapping rate for divacancies by a factor of 2 compared to Fz-Si at room temperature. This should have resulted in a like increase in the trapping rate at low temperatures, but in fact slightly lower values are found and there is even a downward trend below 50 K (Fig. 1) when compared to oxygen-free Si. Kawasuso and Okada[22] found a similar effect below 50 K.

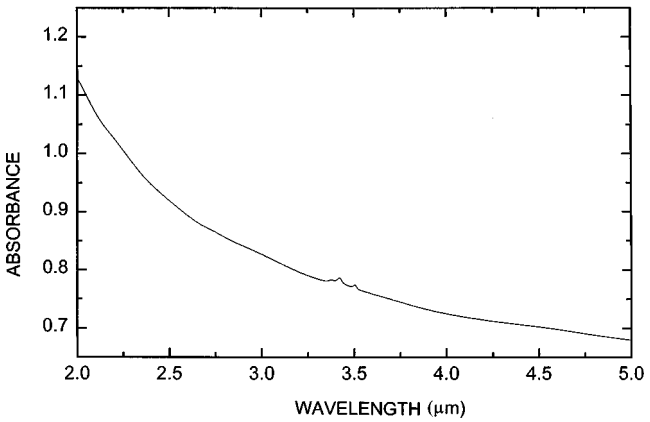

FIG. 10. Optical absorption for the B3 sample. No evidence for an absorption band at 3.9 μm could be found. The change in absorption between 2 and 5 μm is due to scattering from the samples and the sharp absorptions are not related to the samples.

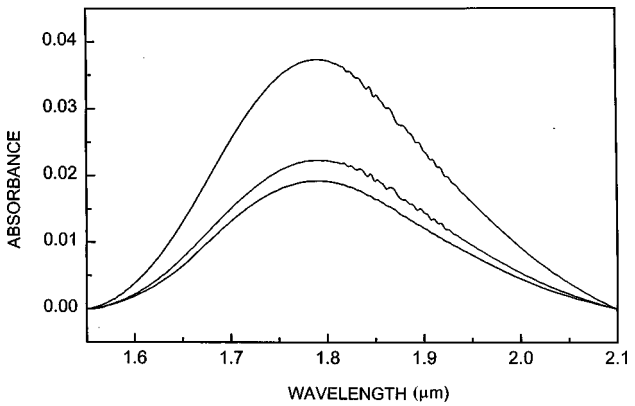

FIG. 11. Optical absorption of the 1.8-μm band for the B3 sample (top curve), the P3 sample (middle curve), and the B0 sample (lower curve). The sharp absorption patterns are due to water vapor present in the ambient atmosphere.

This discrepancy likely arises from (neutral) A centers that give rise to the 830-cm^{-1} infrared absorption band. Two mechanisms can be envisaged: (i) The neutral A centers act as positron traps but only at low temperatures, i.e, they are shallow traps. The consequence would be that at low temperatures an additional lifetime component should emerge with a lifetime close to that for the bulk (217 ps). However, no such additional lifetime could be found nor was one required insofar that adequate fitting was possible without such a component [$\chi^2=1.06\pm0.05$ and a bulk lifetime calculated from Eq. (3) of 217 ± 3 ps]. (ii) The neutral A centers are not shallow traps but modify the Fermi level relative to its position in Fz-Si. This is certainly possible since the A centers have a $0/-$ level situated at $E_c-0.18$ eV, where E_c is the bottom of the conduction band, and their concentration is about $10^{17}/cm^3$. In addition E centers (P V), which have a $0/-$ level at $E_c-0.4$ eV, could also play a role since the divacancy has a $0/-$ charge level close to $E_c-0.5$ eV. One can therefore expect that in such a situation only small changes in the Fermi level with temperature coupled with the temperature dependence of the Fermi distribution can significantly change the balance between $V_2{}^0$ and $V_2{}^-$ concentrations. Thus one may explain the lesser response from divacancies in the P1, P2, and B0 samples by a Fermi-level effect causing more $V_2{}^0$ that trap positrons much less effectively than $V_2{}^-$; essentially this means that the Fermi level is very close to the $0/-$ charge level for the divacancy. We favor this latter explanation because it does not require a new lifetime as does the first one. Furthermore, the differences be-

TABLE IV. Relative strength (to Fz-Si) of the 1.8-μm absorption band and trapping rates from positron measurements. The trapping rate for the Fz-Si sample is 0.65 ± 0.1 ns^{-1}. Data pertain to room temperature.

Sample code	Relative strength (1.8 μm)	Relative strength (±0.2) (trapping rate)
P3	1.5	1.8
B0	1.3	2.0
B3	2.5	1.0

tween the trapping rates below 100 K for the P1, P2, vis-à-vis the B0 sample can be explained by subtle differences in the Fermi level. The above should not be construed to mean that *A* centers cannot be shallow traps *per se*, since this was clearly observed in Ref. 11, but rather that negatively charged *A* centers are, whereas neutral ones are not.

The highly doped samples show temperature dependencies quite different from those just discussed, which suggests association of vacancies with dopants. Furthermore, the temperature dependencies of the irradiation-produced lifetime and its trapping rate are dependent on the dopant concentrations as well as on dopant type (again suggestive of vacancy association with dopants), for which reason we need to discuss these samples individually.

For the *n*-type P3 material (5×10^{17} P/cm^3) the trapping rate is independent of temperature (see Fig. 1) indicating a *neutral* defect (screening by free carriers as discussed by Mäkinen *et al.*,[12] plays no role at this P concentration). Since V_2^- was observed in the P1 and P2 samples they would also have been expected in the P3 sample, so the overall neutral charge is explained by association with positively charged P atoms. We note that although the optical 1.8-μm band shown in Fig. 11 has the same peak position as for free divacancies, the full width at half maximum differs by 6–7 % (smaller), suggesting that the divacancies are not free. The above implies that complexes are formed due to migrating monovacancies, *and* that free divacancy production is significantly reduced (by a factor of 10 or more) to render them unobservable even at low temperatures. We suggest this results from a significantly (tenfold) increased recombination with interstitials caused by the high Fermi level.

The temperature dependency of the lifetime (265 ps at 30 K and 300 ps at 300 K, Fig. 1) could be construed to arise from two types of vacancies whose relative trapping rates change with temperature, but this we consider highly improbable because if so, the observed temperature independence of their total trapping rate would require cancellation of the temperature dependencies of the individual trapping rates. We instead propose that only one defect is responsible, i.e., P V_2, and that the way in which the positron probes this defect is temperature dependent. In the case of InAs, Mahony and Mascher[23] suggested a similar effect. Whether the configuration of the three-body defect P V_2 varies with temperature (there are several ways to arrange two vacancies around a P impurity) or whether the positron's probing of an otherwise constant defect structure is temperature dependent cannot be deduced from these experiments. The Doppler data [see Fig. 2(b)] are not of much help in this regard. The S_D/S_B parameter is close to 1.035 and shows a (reversible) abrupt change around 125 K that is not reflected in any change of the lifetime parameters, which suggests that the momentum distribution of the electrons changes without any change in electron density. Although structural details cannot be deduced, the above indicates a structure radically different from the free divacancies, lending qualitative support to the postulated P V_2 complex

For the highly doped P4 sample we recapitulate the Doppler-based argument that essentially complete trapping occurs in this sample. This precludes calculation of the trapping rate as based on lifetime data, but does allow for a rough estimate of $\sim 45\ \mathrm{ns}^{-1}$ from Doppler data. The lifetime of 260 ps and the virtually constant S_D/S_B value of 1.035 suggest a P-monovacancy complex. The charge state of the P *V* complexes is probably negative but is screened by the high concentration of free carriers, as discussed by Mäkinen, Hautojärvi, and Corbel,[13] so that positrons will be trapped by the complexes as if they were neutral.

TABLE V. Results for irradiated ($1.2\times10^{18}e^-$/cm^2 at 10 MeV) samples measured at room temperature (295 K). τ is the irradiation-produced lifetime, κ the associated trapping rate, and S_D/S_B is the characteristic Doppler parameter for the defect type giving rise to τ. Values of S_B are those listed in Table II, thus disregarding the small contribution from grown-in defects.

Sample code	τ ($\pm$7 ps)	κ ($\pm$0.2 ns^{-1})	S_D/S_B ($\pm$0.007)
P1,P2	305	1.5	1.070
P3	290	2.0	1.035
P4	260	>8[a]	1.035
Sb4	285	6.5	1.080
B0	300	1.2	1.060
B3	280$\pm$20	0.8	[b]
B4	305	3.2	1.060
Fz[c]	300	0.7	1.067

[a]This lower limit is based on lifetime data and is a serious underestimate. Doppler data suggest a value of 45 ns^{-1}. The S_D/S_B value is estimated on the basis of this trapping rate.

[b]The trapping rate is too low to permit calculation of a meaningful value for S_D/S_B.

[c]Data from Ref. 16.

The Sb-doped sample is intermediate between the P3 and P4 samples as far as the increase in lifetime with temperature is concerned, and so is its trapping rate. The doping concentration for the Sb4 sample is also between that for the P3 and P4 samples, so we suggest that a mixture of Sb *V* (dominant) and Sb V_2 complexes is present in this sample, both being neutral because of the temperature-independent trapping rate. The data suggest also in the case of Sb V_2 a configuration-dependent lifetime. However, S_D/S_B has a value (1.08) that suggests, contrarily, dominant trapping by divacancies for which reason we propose that the high S_D/S_B value arises because of the Sb impurity. The lower momentum spread of the outer core electrons in Sb as compared to Si will increase S, and this effect could be augmented by a distortion of the positron wave function towards the Sb impurity either chemically (affinity) or by means of lattice distortion.

This concludes the discussion of the results obtained from *n*-type materials, and we now turn to the *p*-type materials. The B0 sample (4×10^{14} B/cm^3) yields results (see Fig. 3) like those for the P1 and P2 samples (see Fig. 1), which is not surprising in view of the low B concentration. The B3 sample shows a temperature-independent trapping rate, and since positively charged vacancies could not be observed by means of optical absorption, we conclude that in this sample free and neutral divacancies were observed. According to Table IV the relative strength of the 1.8-μm band is 2.5 times higher than in Fz-Si, but the relative trapping rates are the same. This indicates that the trapping rate for the neutral divacancies (at room temperature) is 2.5 times less compared

to those negatively charged. This is in very good agreement with an earlier estimate of 3.[11]

For the B4 sample the positron lifetime of 310 ± 10 ps [Fig. 3(a)] is only marginally higher than for negatively charged free divacancies, while the value of S_D/S_B (Fig. 4) is just slightly smaller. These observations suggest that in the B4 sample divacancies are formed by the radiation, but the temperature dependence of the trapping rate is more difficult to interpret. A possible explanation is that at $T\leqslant150$ K, where the trapping rate is constant, screened positively charged free divacancies trap positrons while above this temperature thermally activated trapping occurs additionally at B V_2 complexes (B V complexes are not stable at room temperature[4]). This latter trapping behavior was also found in InP for divacancies[24] and we find in the present case an activation energy of 32 ± 5 meV, slightly less than in the case of InP (50 meV). At room temperature the exponential factor is 0.28, which means that only $(28\pm5)\%$ of the available B V_2 complexes were detected. The trapping rate from B V_2 complexes at room temperature is $1.8\ \mathrm{ns}^{-1}$ ($3-1.2\ \mathrm{ns}^{-1}$, see Fig. 3), which suggests a B V_2 concentration of $10^{17}\times1.8/0.28=(6.5\pm1.2)\times10^{17}/\mathrm{cm}^3$. Including the contribution from $V_2{}^+$ ($1.2\ \mathrm{ns}^{-1}$), this indicates that a total of $(1.5\pm0.2)\times10^{18}$ monovacancies/cm^3 were retained after irradiation, which is close to that for the P4 sample (see next section). In the B3 sample no increase in trapping rate with temperature was observed likely due to the 10 times lower B concentration. The S parameter for $V_2{}^+$ is, according to Fig. 4(b), about 1.045, which is less than that for $V_2{}^-$ (1.067) indicating a broader electron momentum distribution in the case of V_2^+ caused, possibly, by different lattice relaxations.

The above discussions point to fairly simple processes between vacancies and dopants. Free divacancies are virtually unaffected by dopants when their concentration is below $5\times10^{16}/\mathrm{cm}^3$. At higher dopant concentrations ($\approx5\times10^{17}/\mathrm{cm}^3$) association of vacancies with dopants dominates and free divacancy formation is strongly reduced. P V_2 complexes dominate at 5×10^{17} P/cm^3, a mixture of Sb V (dominant) and Sb V_2 at 1×10^{18} Sb/cm^3 and P V complexes at 5×10^{18} P/cm^3 all for a dose of $1.2\times10^{18}e^-/\mathrm{cm}^2$.

The Doppler data corroborate the association of vacancies with dopants by virtue of their modification of S_D/S_B relative to free divacancies, a result that highlights the strength in combining lifetime and Doppler broadening measurements. Recently, Doppler broadening data analyzed in terms of the contribution from high-momentum core electrons have demonstrated that impurities associated with vacancies can also be detected by this approach,[25] but here we have demonstrated that not only can this be done using S, but also that there is no direct correlation between S values and positron lifetimes.

B. Introduction rates

The Cz-Si samples contain bonded oxygen interstitials at a concentration of $(1-2)\times10^{18}/\mathrm{cm}^3$ whereas in the previously investigated Fz-Si (Ref. 16) their concentration was about two orders of magnitude lower. This difference has no obvious influence on the lifetime data for the unirradiated samples (see Table II) but does affect the Doppler parameter S, which for Cz-Si is consistently lower than that for Fz-Si. The reason for this is not entirely clear, but does suggest that some oxygen impurities weakly interact with positrons as proposed earlier.[26]

Since oxygen is known to be a trap for irradiation-produced vacancies (as verified by our IR data for the A center), it is of interest to compare positron results for oxygen-containing and oxygen-free materials. Table V contains room-temperature lifetime and Doppler data for the lightly P-doped P1 and P2 samples, the lightly B-doped B0 sample, and those for oxygen-free undoped Fz-Si. All of these samples have dopant concentrations at least an order of magnitude less than that for the oxygen, which therefore will dominate as a vacancy trap. Data for these four irradiated samples are very similar; the irradiation-produced lifetime is close to 300 ps, the temperature dependencies of the trapping rates are similar (Figs. 1 and 3), and S_D/S_B is close to 1.067. According to Ref. 16 these features suggest that trapping occurs by negatively charged free divacancies.

The only difference between Fz-Si and Cz-Si is that the trapping rate at 293 K is higher in Cz-Si than in Fz-Si by a factor of $\simeq2$, even though the electron doses were the same, so indicating that about twice as many free divacancies are formed in Cz-Si than in oxygen-free Fz-Si. This result is not explainable if divacancies were formed mainly by migrating monovacancies because some would be removed by oxygen (so giving rise to the IR band observed at 830 cm^{-1}), leaving fewer monovacancies to form divacancies as compared to oxygen-free Fz-Si. On the other hand, if divacancies (which are immobile at 293 K) were mainly formed *directly* by the 10-MeV electrons, which is entirely conceivable, the increase in the concentration of divacancies in Cz-Si could be the result of oxygen interstitials, or clusters of oxygen, trapping mobile silicon interstitials, so effecting a reduction in their recombination with the immobile divacancies. Our data are explainable by this mechanism, but since trapping of silicon interstitials by interstitial oxygen is unstable at room temperature,[8] we suggest that oxygen clusters are the traps as also proposed in connection with thermal donor formation.[27]

Influences from dopants become observable when their concentration is at $5\times10^{17}/\mathrm{cm}^3$ or above, i.e., comparable to the oxygen concentration. In Table V are collected room-temperature lifetime and S_D/S_B results for the five highly doped materials (P3, P4, Sb4, B3, and B4). Except for the P4 and Sb4 samples, irradiation-produced lifetimes range between 290 and 305 ps, indicative of trapping by divacancies, while for the P4 and Sb4 samples the 260–275 ps lifetime suggests trapping dominated by monovacancies. Although it is clear that trapping rates increase with dopant concentration in n-type Si, indicating that the dopants trap vacancies (as supported by the IR data shown in Table III) it is also clear that the p-type materials show much smaller trapping rates than the n-type materials. This should not be construed to mean that fewer defects are formed in p-type materials, but rather that the low Fermi level renders defects neutral or positively charged and consequently reduces the trapping rate as mentioned earlier in Sec. II C.

The 260-ps lifetime observed for the P4 sample indicates P V complexes but divacancies are indicated for the P3 sample. We suggest this difference to be caused by the level of radiation damage *relative* to the dopant concentrations. In the P3 sample the dose produced enough monovacancies for

the P dopants to become associated mainly with divacancies (P V_2), whereas in the P4 sample the ten times higher P concentration is sufficiently large to ensure trapping of mobile monovacancies in the form of P V complexes.

In the case of the P3 sample one might hence expect a distribution of P V, P V_2, P V_3, etc. complexes, and this cannot be ruled out because the various lifetimes arising from such complexes would not be resolvable, but the 290 ps does at least indicate a dominance of the P V_2 complex. The trapping rate of 2 ns^{-1} suggests a divacancy concentration of $\sim 2\times10^{17}/cm^3$, i.e., $\sim 4\times10^{17}/cm^3$ monovacancies according to the calibration between concentration and trapping rate from Refs. 11 and 14 for neutral vacancies (1×10^{17} ns^{-1} cm^3); this yields an introduction rate of 0.4 cm^{-1}.

For the P4 sample the maximum monovacancy concentration would be $5\times10^{18}/cm^3$ (in the form of P V). The minimum trapping rate, as estimated from the Doppler data, was 45 ns^{-1}, which gives a monovacancy concentration of $4.5\times10^{18}/cm^3$. This yields an introduction rate of 3.7–4.2 cm^{-1}. The narrow range is probably fortuitous because of the uncertainty in doping concentration at such a high level as well as in the calibration between trapping rate and concentration. Nevertheless, the estimated introduction rates are large—even ten times larger than that for the P3 sample—but smaller than the theoretical value[9] of 8 cm^{-1} as calculated for relativistic 10-MeV electrons according to the Kinchin-Pease approximation for multiple scattering, which does not take into account any recombination between vacancies and interstitials.

For the P4 sample there is some uncertainty associated with the value of the trapping rate since it is based only on the evidence for saturation of S, see Fig. 7(a). The ensuing estimate of 45 ns^{-1} is, however, not seriously at odds with the extrapolated trapping rate based on the Sb-doped sample (1×10^{18} Sb/cm^3), which showed a trapping rate of 6.5 ± 0.5 ns^{-1}, so suggesting the five times higher P concentration would yield 30–35 ns^{-1}. Basing the extrapolation on the P3 sample instead, a trapping rate of $2\times10\times(1.9\pm0.2)$ $ns^{-1}=34$–42 ns^{-1} is obtained, where the factor 2 arises because divacancies were formed in the P3 sample and the factor 10 arises from the increase in P concentration between the P3 and P4 samples. The above considerations are, obviously, estimative but they do support the ansatz that impurities (P, Sb) at high concentrations dominate as vacancy traps.

Although it is reasonable that increasing the dopant concentration would cause an increase in the *probability* of trapping mobile monovacancies, that by itself does not ensure a larger final vacancy concentration because recombination with interstitial silicon atoms could still occur regardless of whether the vacancies are complexed or not. The increase in vacancy concentration hence points to a decrease in the recombination efficiency between complexed vacancies and interstitials, and a likely source therefore is Coulombic repulsion between these defects. We do point out that the mechanism of reduced vacancy interstitial recombination, here advocated to explain the increase in impurity-vacancy formation, does not apply to free divacancies. The P3, Sb4, and P4 samples showed no effect from free divacancies, which would have been negatively charged in these samples, suggesting that recombination with (at least) one of the interstitials in close proximity to the divacancy is very effective in heavily doped n-type materials.

At present it is an open question as to what then happens to those interstitials that do not recombine with vacancies. Oxygen impurities have formerly been suggested as traps, and in the present paper oxygen is found to cause a twofold increase in the introduction rate of free divacancies, but this is far too small to explain the very large P V, P V_2, Sb V (or Sb V_2) introduction rates. We suggest, therefore, that external surfaces become the main trap for the interstitials when recombination with vacancies is prevented by Coulombic repulsion.

We summarize in Table VI the salient points of the discussions so far by listing the proposed vacancy complexes for the various samples and the introduction rate for *monovacancies*. This presentation of the introduction rate has the advantage in showing how many monovacancies are retained per unit of dose regardless of them being in the form of monovacancies or divacancies. Note that account has been taken of the fact that negatively charged vacancies are detected by positrons three times more effectively (at room temperature) than neutral ones. The ''comments'' column contains remarks important to the differences arising from the dopings.

C. Location dependencies

All data discussed so far pertain to samples cut from the end of the bars that faced the electron beam. In this section we discuss data obtained from various locations on the sample bars. As mentioned in Sec. III, the electron energy decreases from 10 MeV at the front end to an average value of about 2.5 MeV at the far end (27-mm location), and the dose decreases by $\simeq 50\%$. It should be noted that the average 2.5-MeV electron energy is somewhat misleading since it includes electrons with energies too small to cause damage. The most probable energy is $\simeq 3$–4 MeV. From Figs. 5 and 8 we can conclude that the same defect types are created in the ≈ 2.5–10-MeV range as based on the essentially constant lifetimes. The smooth decrease in dose is reflected in the decrease of the trapping rate [see Fig. 5(b)] and we note, incidentally, that this behavior shows that the charge of the defects is the same from one end of the sample to the other.

In the case of the Sb4 sample the temperature dependencies of the lifetime data for the front and back end of the sample bars are very much the same (Fig. 6). Because of the relatively high trapping rate for this sample, lifetime values are determined well enough at the two positions to make possible a distinction between their temperature dependencies. The weaker temperature dependence as well as the lower lifetime values for the 27 mm location suggest that fewer Sb V_2 complexes are formed at the end of the sample bar relative to the Sb V complexes, which is entirely to be expected, i.e., the Sb V_2 complex contributes with a temperature dependence like that for the P3 sample discussed in Sec. IV A.

The S parameters [Figs. 7(a) and 9(a)] decrease as a function of position in all cases *except* for the P4 sample in Fig. 7(a). It is on this latter observation we base our earlier mentioned assumption that complete trapping (at least to within 90%) occurs in the P4 sample.

TABLE VI. Summary of properties of vacancy-type defects in Cz-Si and Fz-Si irradiated with 10-MeV electrons to a dose of $1.2\times10^{18}e^-/\mathrm{cm}^2$.

Sample code	Vacancy complex[a]	Introduction rate[b] (cm^{-1})	Comments
P4 5×10^{18} P/cm^3	PV^-	$\simeq4$	Charge is probably negative but is screened by free carriers[c]
Sb4 1×10^{18} Sb/cm^3	$SbV^0/SbV_2{}^0$	0.6	Indication for thermally activated trapping by $SbV_2{}^0$
P3 5×10^{17} P/cm^3	$PV_2{}^0$	0.4	Temperature-dependent configuration
P2 5×10^{16} P/cm^3	$V_2{}^-$	0.08	A[d] and E[e] center-induced charge change of $V_2{}^-$ toward $V_2{}^0$ at $T<50$ K
P1 2×10^{16} P/cm^3	$V_2{}^-$	0.06	As for the P2 sample
B0 4×10^{14} B/cm^3	$V_2{}^-$	0.05	As for the P2 sample except for E center contribution
B3 5×10^{17} B/cm^3	$V_2{}^0$	0.06	
B4 5×10^{18} B/cm^3	$V_2{}^+/BV_2$	1.1–1.4	Screening of $V_2{}^+$ by free carriers. Thermally activated trapping by BV_2 (of unknown charge)
Fz-Si Undoped	$V_2{}^-$	0.03	Trapping by free $V_2{}^-$

[a]Overall charge is indicated by superscripts.
[b]Introduction rates pertain to monovacancies.
[c]Mäkinen, Hautojärvi, and Corbel (Ref. 13).
[d]A center is substitutional oxygen.
[e]E center is PV.

V. CONCLUSION

Irradiation to a dose of $1.2\times10^{18}e^-/\mathrm{cm}^2$ of a set of variously doped Czochralski silicon samples has shown that free and negatively charged divacancies dominate as positron traps as long as the dopant concentration is less than $5\times10^{16}/\mathrm{cm}^3$, although at low temperatures a shift toward neutral divacancies takes place. This shift is proposed to be a Fermi level effect probably caused by A centers (and possibly E centers in P-doped materials), rather than competitive trapping by positron traps active at low temperatures.

Oxygen impurities increase the free divacancy concentration by roughly a factor of 2 relative to oxygen-free Si, an effect that we suggest is caused by silicon interstitials being trapped by oxygen clusters. P doping at $5\times10^{17}/\mathrm{cm}^3$ increases significantly the amount of divacancies trapped by P impurities and this increase is also ascribed to a reduction in the recombination with interstitials. The structure of the proposed P V_2 defect might be temperature dependent or, alternatively, the localization of the positron at this defect is temperature dependent. P doping at $5\times10^{18}/\mathrm{cm}^3$ further increases the amount of trapped vacancies but in this case P V complexes dominate. A very large introduction rate ($\simeq4\ \mathrm{cm}^{-1}$) is estimated, which approaches the theoretical limit of $\sim8\ \mathrm{cm}^{-1}$, i.e., heavily P-doped Si is very sensitive to irradiation. No free divacancies could be observed in the two heavily P-doped materials, suggestive of strong recombination between the two interstitials and two vacancies when the Fermi level is high.

The heavily B-doped sample (B3) showed trapping by neutral divacancies while for the most heavily doped B4 sample evidence was found for thermally activated trapping by B V_2 complexes and trapping by screened positively charged divacancies.

The S_D/S_B parameters for impurity-trapped vacancies can be significantly different from that for free negatively charged divacancies (1.067). Sb V (dominant)/V_2 has a larger value (1.080), P V_2 a lower value (1.035), and B V_2 has nearly (1.060) the free-divacancy value. For P V, S_D/S_B is 1.035 and for $V_2{}^+$ is 1.045.

Defect structures are not materially influenced by electron energies ranging between ≈2.5 and 10 MeV, or by doses varying between $\sim0.6\times10^{18}/\mathrm{cm}^2$ and $1.2\times10^{18}/\mathrm{cm}^2$.

ACKNOWLEDGMENTS

This work was financially supported by the Natural Sciences and Engineering Research Council of Canada. We are indebted to Dr. S. Hahn for supplying the Cz samples and to Dr. C. Ross, NRCC, Ottawa, for performing the electron irradiation. The assistance of J. Wang, NRCC, Winnipeg, in connection with the infrared absorption measurements, is gratefully acknowledged.

[1] G. D. Watkins and J. W. Corbett, Phys. Rev. A **138**, 543 (1965).
[2] J. W. Corbett and G. D. Watkins, Phys. Rev. A **138**, 555 (1965).
[3] E. G. Sieverts, S. H. Muller, and C. A. J. Ammerlaan, Solid State Commun. **28**, 221 (1978).
[4] G. D. Watkins, Phys. Rev. B **13**, 2511 (1976).
[5] M. Sprenger, R. van Kemp, E. G. Sieverts, and C. A. J. Ammerlaan, Phys. Rev. B **35**, 1582 (1987).
[6] Young-Hoon Lee and J. W. Corbett, Phys. Rev. B **13**, 2653 (1976).
[7] Young-Hoon Lee, N. N. Gerasimenko, and J. W. Corbett, Phys. Rev. B **14**, 4506 (1976).
[8] H. J. Stein, Radiat. Eff. **22**, 169 (1974).
[9] J. W. Corbett, in *Solid State Physics Suppl. 7*, edited by H. Ehrenreich, F. Seitz, and D. Turnbull (Academic, New York, 1966), p. 20.
[10] J. L. Lindström and B. G. Svensson, in *Oxygen, Carbon, Hydrogen, and Nitrogen in Crystalline Silicon*, edited by J. C. Mikkelsen, Jr. *et al.*, MRS Symposia Proceedings No. 59 (Materials Research Society, Pittsburgh, 1986), p. 45.
[11] P. Mascher, S. Dannefaer, and D. Kerr, Phys. Rev. B **40**, 11 764 (1989).
[12] J. Mäkinen, C. Corbel, P. Hautojärvi, P. Moser, and F. Pierre, Phys. Rev. B **39**, 10 162 (1989).
[13] J. Mäkinen, P. Hautojärvi, and C. Corbel, J. Phys.: Condens. Matter **4**, 5137 (1992).
[14] A. Kawasuso, M. Hasagawa, M. Suezawa, S. Yamaguchi, and K. Sumino, Jpn. J. Appl. Phys., Part 1 **34**, 2197 (1995).
[15] T. Chiba, A. Kawasuso, M. Hasegawa, M. Suezawa, T. Akahane, and K. Sumino, Mater. Sci. Forum **175-178**, 327 (1995).
[16] V. Avalos and S. Dannefaer, Phys. Rev. B **54**, 1724 (1996).
[17] R. N. West, Adv. Phys. **22**, 263 (1973).
[18] S. Dannefaer and D. Kerr, Phys. Rev. B **50**, 14 096 (1994).
[19] S. Dannefaer and T. Bretagnon, J. Appl. Phys. **77**, 5584 (1995).
[20] International Commission on Radiation Units and Measurements (ICRU) Report No. 35, 1984 (unpublished); ICRU Report No. 37, 1984 (unpublished).
[21] L. J. Cheng, J. C. Corelli, J. W. Corbett, and G. D. Watkins, Phys. Rev. **152**, 761 (1966).
[22] A. Kawasuso and S. Okada, Jpn. J. Appl. Phys., Part 1 **36**, 605 (1997).
[23] J. Mahony and P. Mascher, Phys. Rev. B **55**, 9637 (1997).
[24] T. Bretagnon, S. Dannefaer, and D. Kerr, J. Appl. Phys. **81**, 3446 (1997).
[25] U. Myler, R. D. Goldberg, A. P. Knights, D. W. Lawther, and P. J. Simpson, Appl. Phys. Lett. **69**, 3333 (1996).
[26] S. Dannefaer and D. Kerr, J. Appl. Phys. **60**, 1313 (1986).
[27] D. Mathiot, Appl. Phys. Lett. **51**, 904 (1987).